J. theor. Biol. (2002) **216,** 147–158
doi:10.1006/yjtbi.2551, available online at http://www.idealibrary.com on IDEAL®

A Mathematical Model of Pattern Formation in the Vascular Cambium of Trees

ERIC M. KRAMER*

Physics Department, *Simon's Rock College*, 84 *Alford Road*, *Great Barrington*, *MA*01230, *U.S.A.*

(*Received on* 18 *September* 2001, *Accepted in revised form on* 29 *January* 2002)

The beautiful patterns apparent in wood grain have their origin in the alignment of fusiform initial cells in the vascular cambium of trees. We develop a mathematical model to describe the orientation of fusiform initial cells, and their interaction with the plant hormone indole-3-acetic acid (auxin). The model incorporates the following four assumptions: (1) auxin is actively transported parallel to the long axis of the initials, (2) auxin diffuses perpendicular to the long axis of the initials, (3) the initials tend to orient parallel to the flux of auxin through the cambium, and (4) adjacent initials tend to orient parallel to one another. Each assumption is justified on the basis of available evidence and cast in mathematical form. Our main result is a pair of nonlinear differential equations that describe the coupling between the distribution of auxin in the cambium and the orientation of fusiform initials. Numerical solutions to the equations show qualitative resemblance to the wood grain patterns observed at branch junctions, wounds and knots, and topological defects.

Introduction

A tree branch grows in diameter through the action of the vascular cambium, a layer of tissue only one cell thick that forms a continuous cylindrical sheath around the wood of the branch (Iqbal, 1990; Romberger *et al.*, 1993; Larson, 1994). During active growth, the cambium moves gradually outward, leaving behind layers of daughter cells that differentiate into the various xylem elements that constitute new wood. The cambium also produces layers of daughter cells that precede its outward expansion and that differentiate into phloem. Following Wilson *et al.* (1966), the vascular cambium and adjacent layers of developing cells are together called the cambial region. The cambial region is typically less than 1 mm thick.

Of particular interest here are the fusiform initial cells of the vascular cambium. Fusiform initials are elongated cells whose arrangement is reiterated in the mature xylem of the wood. The orientation of the initials thus determines the orientation of wood grain (the general direction of wood anisotropy).†

Since the wood of a branch is formed by the gradual accretion of new xylem at the circumference, serial tangential sections are a standard technique to study the changing organization of fusiform initials (Iqbal, 1990; Romberger *et al.*, 1993; Larson, 1994). Such studies show the

*E-mail: ekramer@simons-rock.edu

† "Wood grain" as discussed here should not be confused with the bands of alternating light and dark-colored wood visible in plane-cut lumber due to the annual growth rings.

0022-5193/02/$35.00/0

cambium to be a surprisingly dynamic tissue. In many tree species, the production of new initials through cell divisions‡ exceeds the capacity of the cambium to accommodate them, leading to the subsequent elimination of some initials. This has led many authors to conclude that initials compete intensely for available space (although the cellular basis of this competition is not clear). In addition, initials may change their orientation rapidly in response to changing stimuli. Harris (1973) cut a spiral girdle from the bark of a *Pinus radiata* stem, and observed that initials near the girdle rotated by about 40° during 9 weeks of subsequent growth.

The plant hormone auxin (specifically, indole-3-acetic acid, abbreviated IAA) plays an important role in the differentiation of vascular tissues (Jacobs, 1952; Sachs, 1969, 1981, 1991, 2000; Zajaczkowski *et al.*, 1984). In trees, auxin is produced by growing shoots and leaves and transported basipetally through the cambial region (Little & Savidge, 1987; Sundberg & Uggla, 1998). A plausible theory for the role of auxin in tree polarity suggests that fusiform initials tend to align parallel to the flux of auxin through the cambium (Harris, 1969, 1973, 1981, 1989; Kirschner *et al.*, 1971; Zagorska-Marek & Little, 1986). The theory is motivated by numerous grafting, and girdling experiments in which an impediment to auxin flow causes a re-orientation of the fusiform initials near the impediment (for a review see chap. 7 in Harris, 1989). Auxin is specifically implicated in these experiments since the application of exogenous auxin can decrease or prevent re-orientation (Harris, 1969; Kirschner *et al.*, 1971; Zagorska-Marek & Little, 1986). The morphological importance assigned to the *flux* of auxin is also well suited to describe the general appearance of wood grain at knots and branch junctions. For example, the presence of circular grain patterns in trees rules out theories based solely on the concentration or the concentration gradient of a hormone (Sachs & Cohen, 1982; Lev-Yadun & Aloni, 1990; Kramer, 1999). Of course, the concentration, gradient, and flux of auxin are interrelated. The details of the relationship will be described below.

‡Specifically, anticlinal cell divisions, which tend to increase the number of initials in a tangential section. Periclinal divisions are responsible for radial expansion.

Changing grain angle is not due simply to the rotation of initials. Several cellular processes may contribute, including orientation of new cell walls formed during pseudo-transverse divisions, preferential elimination of initials that are out of parallel with the flux, and re-arrangement of adjacent initials (Kirschner *et al.*, 1971; Harris, 1973; Hejnowicz, 1973; Zajaczkowski *et al.*, 1984; Zagorska-Marek & Little, 1986). Regarding the third process, Harris (1973) presented micrographic evidence that fusiform initials undergoing a change of orientation tend to adopt a sigmoid shape so that their apical tip points "up-stream" of the auxin flux and their basal tip points "down-stream". He speculated that the body of the initial would gradually rotate to lie parallel to the tips.

In this paper, we set the theory of auxin-mediated cambial orientation in mathematical form and examine some of its consequences for wood grain patterns. The model presented here neglects the potentially important roles of mechanical stresses (Mattheck & Kubler, 1995; Green, 1999), of water and nutrient availability, of other growth factors like ethylene and gibberellins (Little & Pharis, 1995), and of genetic influences (Savidge, 1996). We are limiting consideration to auxin flux as a first approximation, to show the wide range of phenomena that may be understood in these limited terms.

Model of Auxin Transport

TRANSPORT IN ONE DIMENSION

The best available mathematical model of auxin transport was developed by Mitchison (1980) and Goldsmith, Goldsmith & Martin (1981), henceforth called the MGGM model. Both papers consider the chemiosmotic transport of auxin (Rubery & Sheldrake, 1974; Raven, 1975; Goldsmith, 1977; Lomax *et al.*, 1995) through a single, homogeneous column of meristematic cells aligned end to end.

The MGGM model includes three contributions to the flux of auxin across the cell membrane: export of auxin anion (IAA^-) via a membrane-bound efflux carrier, passive diffusion of IAAH through the cell membrane, and

import of IAAH via a membrane-bound uptake carrier. The polarity of auxin transport is due to the localization of the auxin efflux carrier to the basal end of the cell (Mitchison, 1980; Goldsmith *et al.*, 1981; Jacobs & Gilbert, 1983). Since the publication of MGGM, Lomax *et al.* (1985) demonstrated that auxin import is an active process, involving the transport of two protons with each auxin anion. The details of MGGM must be corrected to account for this, but the important result for our purposes, eqn (1) below, is unchanged.

MGGM treats auxin concentration as a function of position within the cell, with discontinuous jumps at semi-permeable membranes [see Fig. A1]. This should be compared to the spatial resolution of typical transport experiments, which measure the concentration of radio-labeled auxin in stem segments 2–10 mm in length (Hollis & Tepper, 1971; Zamski & Wareing, 1974; Little, 1981; Lachaud & Bonnemain, 1982, 1984; Odani, 1985). It is instructive to rewrite the model of MGGM in terms that are directly comparable to transport experiments. This requires the introduction of a quantity that averages the concentration of auxin over large lengths compared to one cell. We call this the *smoothed* auxin concentration, C.

In terms of the smoothed auxin concentration, the MGGM model reduces to the usual equation describing the flux of a solute under the combined action of transport and diffusion (Benedek & Villars, 2000)

$$J = -D_{eff}\,\frac{\mathrm{d}C}{\mathrm{d}x} + vC, \qquad (1)$$

where J is the auxin flux, D_{eff} is the effective diffusion constant, and v is the velocity of active transport (derivation in Appendix A). The MGGM model also assumes that auxin is neither synthesized nor immobilized in the transport pathway, i.e. auxin is conserved during transport (the validity of this assumption for trees is discussed below). The continuum statement of conservation is the one-dimensional *continuity equation*

$$\frac{\partial C}{\partial t} = -\frac{\partial J}{\partial x}, \qquad (2)$$

which relates the flux of auxin into a region to the rate of auxin increase. Analytic and simulation results of the continuum model, as described by eqns (1) and (2), are indistinguishable from the results of MGGM.

Values for D_{eff} and v may be calculated from the known membrane permeabilities, compartment pHs, etc. (see Appendix A), or they may be estimated from the distribution of radio-labeled auxin measured in transport experiments (Hollis & Tepper, 1971; Zamski & Wareing, 1974; Little, 1981; Lachaud & Bonnemain, 1982,1984; Odani, 1985). Experimentally determined transport velocities range from 0.5–1.5 $\mathrm{cm\,hr^{-1}}$, and our estimates of D_{eff} based on published radio-label profiles fall in the range 0.04–0.09 $\mathrm{cm^2\,hr^{-1}}$. The model predictions of Goldsmith *et al.* (1981) for velocity fall in the correct range, but the effective diffusion constant is significantly too low, $D_{eff} = 0.005-0.014\,\mathrm{cm^2\,hr^{-1}}$§. We mentioned above that the MGGM model requires some correction. This could increase the model prediction for D_{eff}, but even so it could not exceed the diffusion constant for auxin in water, $D = 0.024\,\mathrm{cm^2\,hr^{-1}}$ (Mitchison, 1980). To explain the remaining discrepancy between model and experiment, note that a transverse section through the cambial region intersects thousands of adjacent pathways for auxin transport. Any inhomogeneity among the transport pathways (e.g. a range of cell lengths) will cause a pulse of radio-labeled auxin to spread faster than predictions based on a single column of homogeneous cells, resulting in a larger effective diffusion constant. Typical transport experiments also average the data from multiple specimens, further increasing the inhomogeneity of the transport pathways.

THE CAMBIAL SURFACE

In two recent papers (Kramer, 1999, 2001), we have argued for the utility of an approach that approximates the cambial region of a tree as a curved surface of negligible thickness, henceforth referred to as the *cambial surface*. All

§ Values for D_{eff} were calculated following the analysis in Appendix A [see eqn (A.5)] and checked against the computer simulations of auxin concentration profiles reported in Goldsmith *et al.* (1981).

relevant quantities are then defined as integrals or averages through the thickness of the cambial region. This approach allows us to simplify the problem of morphogenesis from three dimensions to two. The distribution of auxin in the cambial surface, denoted m, thus has units of mass per unit area. The flux of auxin tangent to the cambial surface, denoted $\mathbf{j}$, is a vector with units of mass through unit length per unit time.

In the previous section, it was helpful to introduce the smoothed auxin concentration, C. We define the auxin distribution $m(x, y)$ and flux $\mathbf{j}(x, y)$ to be similarly smoothed quantities, averaged over a tangential area of 1 mm^2 in the neighborhood of the point (x, y). This area is large enough to include dozens to hundreds of cambial cells, depending on the thickness of the cambial region. Both m and $\mathbf{j}$ may thus be treated as smoothly varying functions of position on the cambial surface.

We use a third smoothed quantity to describe the orientation of cells in the cambial region. This is the grain direction, $\mathbf{u}(x, y)$, a unit vector tangent to the cambial surface [see Figs 1(a) and (b)]. In practical terms, the grain direction is the direction of cracks and striations visible at the surface of a debarked log and in tangential wood sections. In terms of the underlying cambial cells, the grain direction may be defined as the vector average over basipetal orientations of cambial initials in a region of size 1 mm^2. The use of a smoothed field to represent grain direction permits us to model the orientation of cambial cells in aggregate, rather than individually.

In this paper, we limit consideration to cambial surfaces that are either flat or portions of a cylinder. This allows us to use undergraduate vector calculus. More general curved surfaces would require the use of differential geometry (Morgan, 1998). We will also exclude from consideration tree species with large aggregate rays, since a ray wider than about 1 mm represents a discontinuity in $\mathbf{u}$.

TRANSPORT IN TWO DIMENSIONS

Due to the basal localization of the auxin efflux carrier (Mitchison, 1980; Goldsmith *et al.*, 1981; Jacobs, 1983), the active transport of auxin is parallel to the long axis of transporting cells. A generalization of eqn (1) for the auxin flux through the cambial surface is therefore only applicable to the flux component parallel to the local grain direction. We write

$$j_{\parallel} = -D_{\parallel} \nabla_{\parallel} m + vm, \tag{3}$$

where $\nabla_{\parallel} m = \mathbf{u} \cdot \nabla m$ and the subscript "$\parallel$" denotes quantities measured parallel to the local grain direction. This component of the auxin flux is shown schematically in Fig. 1(c).

We also need to specify the component of auxin flux perpendicular to the grain direction. To our knowledge there have been no experimental studies of this quantity. However, some theoretical insight can be gained from the MGGM model. Omitting the contribution of the basal efflux carrier responsible for active transport, and repeating the analysis described in Appendix A, we find that the flux perpendicular to the grain is diffusive,

$$j_{\perp} = -D_{\perp} \nabla_{\perp} m, \tag{4}$$

where the subscript "$\perp$" denotes quantities measured perpendicular to the grain. This component of the auxin flux is shown schematically in Fig. 1(d). The effective diffusion constant $D_{\perp}$ is predicted to be smaller than $D_{\parallel}$ by a factor of between 3 and 10. This result is easy to understand considering that cell membranes are the main barrier to diffusion of the auxin anion (IAA^-). Since cambial cells are typically 10–20 times longer than they are wide (Iqbal, 1990; Romberger *et al.*, 1993; Larson, 1994), it is proportionately easier for auxin to diffuse parallel to the grain.

Although we know of no direct measurements of transverse diffusion in trees, it is an unavoidable corollary of the chemiosmotic theory (Mitchison, 1980; Goldsmith *et al.*, 1981; Rubery & Sheldrake, 1974; Raven, 1975; Goldsmith, 1977; Lomax *et al.*, 1995) and supported by experiments in herbaceous species. In his analysis of geotropism experiments in shoots, Mitchison (1981) estimated that 25% of the auxin that leaves a cell does so through the side walls. Similarly, Sachs' discussion of experiments that manipulate the polarity of plant stem tissues relies on the ability of auxin to diffuse transverse to the plant axis (Sachs, 1981, 1991). He writes

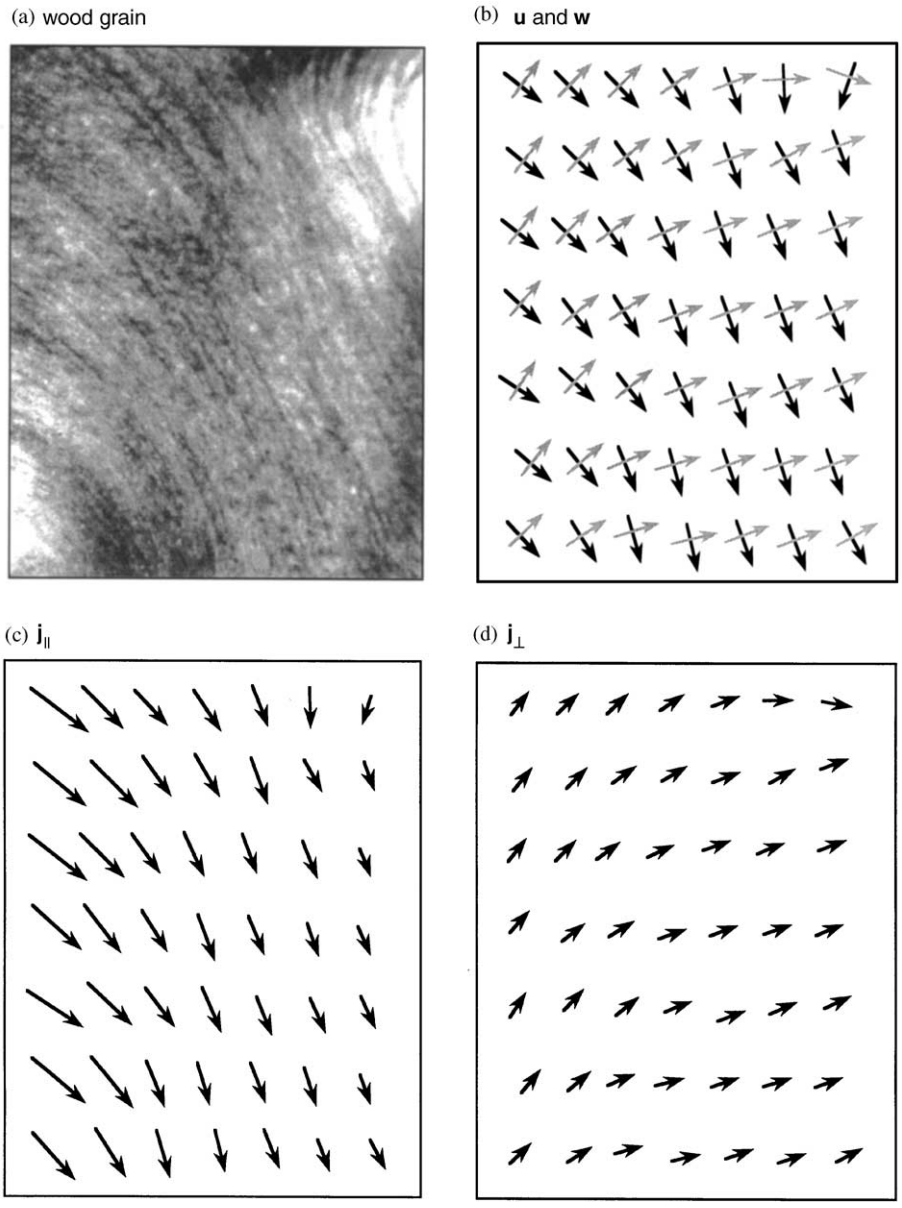

FIG. 1. Schematic illustration of the vector fields discussed in the paper. (a) Digital image of wood grain on the surface of a debarked cottonwood (*Populus deltoides*) log. The section shown is about 4 mm wide. (b) The associated grain direction field **u**, drawn by eye, is shown in black. The perpendicular vector field **w** is shown in gray. Both **u** and **w** are defined to have unit length. (c) The component of the auxin flux parallel to the grain direction, $j_{\|}$, drawn for the hypothetical situation that the concentration of auxin is much larger near the left edge of the image. This component is mainly due to active transport by the cambial cells. (d) The component of auxin flux perpendicular to the grain direction, $j_{\perp}$, also drawn for the hypothetical situation that the concentration of auxin is much larger near the left edge of the image. As discussed in the text, this component is essentially diffusive and will typically be much smaller than $j_{\|}$. Over time, the grain direction will rotate in the direction indicated by $j_{\perp}$. The total auxin flux at any point is the vector sum of $j_{\|}$ and $j_{\perp}$.

that the polarity changes "wherever auxin accumulates and diffuses passively through competent tissues" (Sachs, 2000). In trees, the action of transverse diffusion is consistent with observations of a uniform auxin distribution around the circumference of *Pinus sylvestris* stems (Sundberg *et al.*, 1991; Uggla, 1998).

The description of transverse diffusion requires the introduction of a vector field **w**, defined to be everywhere perpendicular to the

local grain direction, **u** [see Fig. 1(b)]. Then, $\nabla_\perp m = \mathbf{w}\cdot\nabla m$ and the net auxin flux is the vector sum of eqns (3) and (4),

$$\mathbf{j} = [-D_\parallel \nabla_\parallel m + vm]\mathbf{u} + [-D_\perp \nabla_\perp m]\mathbf{w}. \quad (5)$$

To specify the time evolution of the auxin distribution, we also need the two-dimensional continuity equation

$$\frac{\partial m}{\partial t} = -\nabla\cdot\mathbf{j} = -\frac{\partial j_x}{\partial x} - \frac{\partial j_y}{\partial y}, \quad (6)$$

which relates the rate of auxin increase to the flux of auxin into a region. In principle, eqn (6) could include additional terms representing the rates of auxin synthesis and immobilization in the cambial region. However, as discussed in Kramer (2001), these factors are only significant for auxin transport over intra-cambial distances larger than the diameter of the branch. In this paper, we limit consideration to transport over distances of a few centimeters, so we can safely neglect such terms here.

Model of Cambial Orientation

The theory that fusiform initials rotate until they are parallel to the auxin flux requires that initials be sensitive to flux perpendicular to the grain direction (Sachs, 1981, 1991, 2000; Harris, 1969, 1973, 1981, 1989). Referring to eqn (4), we see that the transverse flux of auxin is diffusive. Thus, the initials do not need to sense auxin flux *per se*, but only the transverse gradient that gives rise to the flux. The reader may question as to whether the gradient of auxin across the width of a cambial initial, typically 20–40 μm (Iqbal, 1990; Romberger *et al.*, 1993; Larson, 1994), is large enough to have a biological effect. This is a question to be addressed by experiment, but we mention here that some chemotactic cells are sensitive to chemical gradients as small as 1% per 25 μm (Baier & Bonhoeffer, 1992; Parent & Devreotes, 1999).

We seek an equation describing the time rate of change of the grain direction field **u**. When working with a unit vector field like **u**, it is frequently more convenient to discuss the angle field $\phi(x, y)$, defined in Cartesian coordinates by $\phi = \tan^{-1}(u_y/u_x)$. Then, $\mathbf{u} = \cos(\phi)\mathbf{x} + \sin(\phi)\mathbf{y}$ and $\mathbf{w} = -\sin(\phi)\mathbf{x} + \cos(\phi)\mathbf{y}$. In terms of ϕ, the simplest equation one may write for the auxin-mediated theory of cambial orientation is

$$\left.\frac{\partial\phi}{\partial t}\right|_{auxin} = -\mu\nabla_\perp m, \quad (7)$$

where we have assumed a linear dependence on the gradient for simplicity and μ is a proportionality constant. This equation says the grain direction **u** will rotate until it is pointing downstream of the auxin flux.

Note that eqn (7) cannot be strictly correct since m is the auxin concentration integrated across the thickness of the cambial region, while the fusiform initials occupy only a fraction of the total thickness. However, it is adequate for our purposes if the concentration of auxin at the position of the fusiform initials is roughly proportional to m. Analysis of the data reported in Uggla *et al.* (1998) for the radial distribution of auxin in the cambial region of *Pinus sylvestris* supports this assumption.

Computer simulations taking eqn (7) as the equation of motion for the grain direction yield unrealistic grain patterns, including the rapid and irreversible formation of sharp kinks. To generate more realistic grain patterns, it is necessary to include an additional term whose effect is to smooth out the grain angle with time. Rather than introduce this term *ad hoc*, we would like to argue for the plausibility of such a term by analogy with the physics of liquid crystals.

Liquid crystals are solutions of rod-shaped molecules with properties intermediate between those of a liquid and a crystal (De Gennes, 1995). Relevant for our discussion is the nematic phase, in which the molecules are free to move about in solution, but their rotational freedom is severely constrained due to frequent collisions with adjacent molecules. As a result, molecules in the nematic phase spontaneously adopt an approximately parallel arrangement. Theories explaining the nematic phase require only that the particles are sufficiently long (length-to-width ratios greater than 3 : 1) and densely packed (Onsager, 1949; Vroege & Lekkerkerker, 1992). Attractive intermolecular forces may be present, but do not play a critical role. In this

sense, *crowding* suppresses fluctuations in the orientation and causes the molecules to align.

Although intercellular interactions in the vascular cambium are presumably more complicated than the intermolecular forces in a liquid crystal, we suggest that crowding pays a similar role. Excepting the intervening ray initials, the fusiform initials are packed tightly together. The fusiform initials are also elongated, with length-to-width ratios of 10 : 1 or greater (Iqbal, 1990; Romberger *et al.*, 1993; Larson, 1994). Following the standard discussions of nematic liquid crystal dynamics, the effects of crowding on orientation may be written (De Gennes, 1995) as

$$\left.\frac{\partial\phi}{\partial t}\right|_{crowding} = K\nabla^2\phi, \tag{8}$$

where K is an effective diffusion constant for ϕ.‡

The idea that contact-mediated interactions between elongated cells can cause them to align has been elaborated in a series of papers by Edelstein-Keshet and co-workers, who were initially motivated by the alignment of fibroblasts in cell cultures (Edelstein-Keshet & Ermentrout, 1990; Mogilner & Edelstein-Keshet, 1995, 1996). They also discuss the utility and limitations of the analogy with liquid crystals.

The complete equation of motion for the grain angle combines the effects of transverse auxin gradients and crowding,

$$\frac{\partial\phi}{\partial t} = K\nabla^2\phi - \mu\nabla_\perp m. \tag{9}$$

Equations (5), (6) and (9) together constitute our mathematical model of auxin-mediated cambial orientation. We show below that numerical solutions to this model reproduce several qualitative features of cambial orientation in trees.

We expect the parameters in eqn (9) to vary between species. In addition, they may depend on any of the factors known to influence other aspects of tree growth, including water and nutrient availability, other growth hormones, mechanical stresses, etc. In the absence of more complete information about the cellular orientation mechanism, the parameters may be estimated from the results of girdling and grafting experiments. A reliable parameter determination will require the simultaneous measurement of the auxin distribution and the orientation of fusiform initials.

‡ This is the isotropic version. The anisotropic version,

$$\left.\frac{\partial\phi}{\partial t}\right|_{crowding} = K_\parallel\nabla_\parallel^2\phi + K_\perp\nabla_\perp^2\phi$$

is more general, but it represents an unnecessary complication for the present discussion.

Consequences of the Model

In this paper, we limit consideration to static (i.e. time-independent) grain patterns. This is sufficient to examine many qualitative features of the model, and it simplifies the analysis. Setting time derivatives equal to zero, eqns (5), (6), and (9) reduce to

$$0 = \nabla\cdot\{D_\parallel\mathbf{u}\nabla_\parallel m + D_\perp\mathbf{w}\nabla_\perp m - vm\mathbf{u}\}, \tag{10}$$

$$0 = \nabla^2\phi - \frac{\mu}{K}\nabla_\perp m, \tag{11}$$

where we have divided through by K in the second equation. Before discussing the solutions to this pair of equations, it is instructive to consider what happens if the distribution of auxin is approximately constant. Then, the gradient of auxin is negligible and the static equations simplify to $\nabla\cdot\mathbf{u} = 0$ and $\nabla^2\phi = 0$. Both conditions are satisfied by straight and spiral grain on a cylindrical branch, and also by the circle patterns common in whirled grain. In Kramer (1999), the zero-divergence rule was deduced empirically. Here, the rule emerges as a limiting case of the full model.

The governing differential equations for static wood grain patterns, eqns (10) and (11) are nonlinear. An analytic solution for m and ϕ is thus difficult or impossible in most cases of interest. However, one can solve the equations on a computer using standard techniques (Press *et al.*, 1989; also see Appendix B).

All numerical solutions (Figs. 2–5) are calculated on a square lattice of $(120)^2$ points, corresponding to a square section of the cambial surface with dimensions $2.4\,\mathrm{cm}\times 2.4\,\mathrm{cm}$. A flux of auxin with magnitude $j = 50\,\mathrm{ng\,cm^{-1}\,hr^{-1}}$ is supplied at the top edge of the square, and auxin

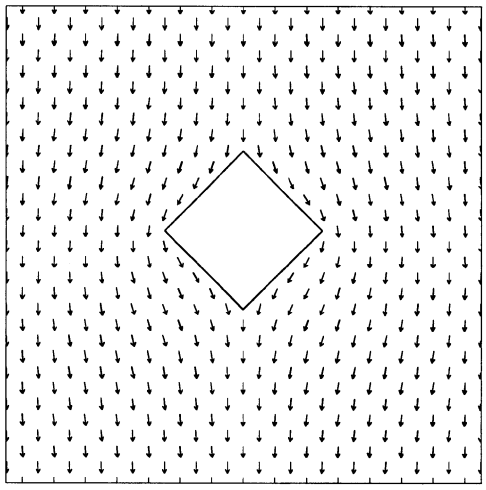

FIG. 2. The grain direction field **u** surrounding a 4 mm × 4 mm hole in the cambium, corresponding to a small knot or wound callus. Total area shown is 17 mm × 17 mm. For clarity, only one lattice site in 16 is decorated with a vector.

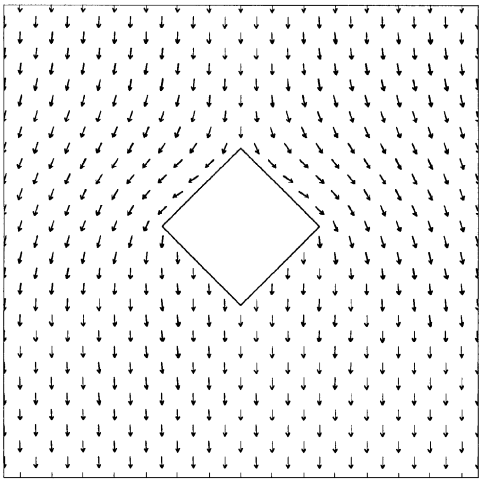

FIG. 4. The grain direction field **u** surrounding a 4 mm × 4 mm branch junction in the cambium. Other parameters same as in Fig. 2.

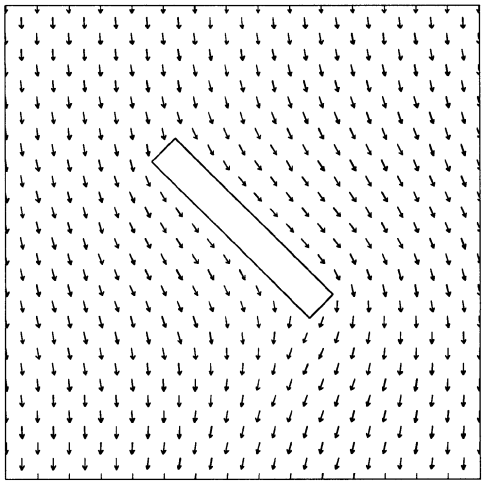

FIG. 3. The grain direction field **u** surrounding a 8 mm × 1 mm diagonal slot in the cambium. Other parameters same as in Fig. 2.

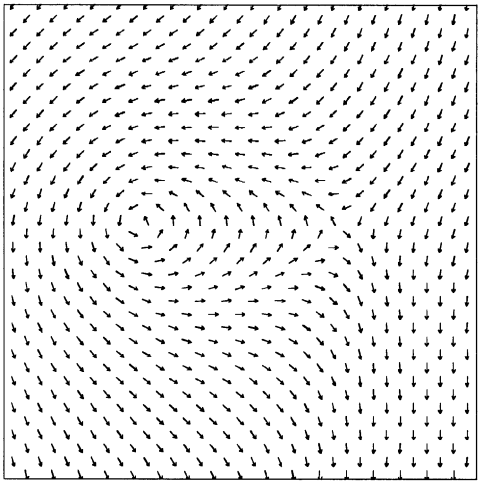

FIG. 5. The grain direction field **u** surrounding a pair of topological defects, specifically a circle pattern (left) and an X-pattern (right). Total area shown is 15 mm × 15 mm.For clarity, only one lattice site in nine is decorated with a vector.

that reaches the bottom of the square is removed. Grain angles at the boundary are fixed to point basipetally. To minimize boundary effects on the calculation of m and ϕ in the interior of the square, impediments to the flux of auxin are placed near the center and are typically less than 1.0 cm in size. The parameter values used for auxin transport are $D_{\parallel} = 0.05\,\mathrm{cm^2\,hr^{-1}}$, $D_{\perp} = 0.01\,\mathrm{cm^2\,hr^{-1}}$, and $v = 1.0\,\mathrm{cm\,hr^{-1}}$. In the equation for grain orientation, the choice $\mu/K = 0.2\,\mathrm{cm\,ng^{-1}}$ gives roughly equal importance to the effects of auxin and crowding.

Figure 2 shows the grain surrounding a square hole in the cambium, corresponding to a knot or wound callus (a square shape is used because it is relatively easy to implement on the square lattice). Note the familiar feature that grain seems to "flow" around the impediment. The

boundary conditions at the edge of the hole are $\mathbf{n}\cdot\mathbf{j}=0$ and $\mathbf{n}\cdot\nabla\phi=0$, where $\mathbf{n}$ is a vector normal to the edge of the hole. The first condition says auxin may not exit the cambium into the hole. The second condition says there is no preferred grain angle for initials adjacent to the edge of the hole. We also considered an alternative boundary condition on ϕ such that initials were constrained to orient parallel to the edge of the hole. A solution with this alternative condition did not differ significantly from the grain shown in Fig. 2.

Figure 3 shows a situation similar to Fig. 2, but with a diagonal slot in the cambium. Note the strong tendency for the grain to orient parallel to the long axis of the slot. This corresponds to the observation that spiral girdling experiments and twining vines can induce the formation of spiral grain in a branch (Harris, 1969, 1973, 1981, 1989; Zagorska-Marek & Little, 1986).

Figure 4 corresponds to a junction where the cambium of a small branch joins the stem along the perimeter of the square hole (imagine a small branch pointing out of the page). To model this circumstance, the perimeter of the junction is a source of auxin flux comparable in magnitude to the auxin flux supplied at the top of the domain. Comparing Figs 2 and 4, we see that auxin produced by the small branch is necessary for the maintenance of grain polarity below the junction. If the auxin flux ceases, the grain will re-orient to the condition shown in Fig. 2, effectively cutting off the branch from supplies of water and solute.

Figure 5 shows a solution with good qualitative resemblance to the associations of circle and X-patterns common in whirled grain (Lev-Yadun & Aloni, 1990; Kramer, 1999). As described in Kramer (1999), these patterns may be classified using standard techniques from the study of inorganic pattern formation (De Gennes, 1995). Specifically, the circle and X-patterns are topological defects with winding number $+1$ and -1, respectively. The solution for the grain direction field was calculated subject to the condition that the cores (i.e. the centers) of the two defects were fixed in place. This result demonstrates that the circle and X-patterns are *stable* solutions to the static equations—they cannot vanish from the cambium unless their cores are free to move. In Kramer (1999), we observed that, of the many possible grain patterns consistent with a topological defect of winding number $+1$, only the circle pattern is observed in whirled grain. The model reproduces this important feature.

Conclusion

In this paper, we present a mathematical model of wood grain development in trees. Auxin is actively transported parallel to the local grain direction, and allowed to diffuse perpendicular to the grain. The fusiform initials tend to orient parallel to the net auxin flux, and also parallel to their neighbors in the vascular cambium.

Since the initials transport auxin longitudinally, and are also sensitive to the transverse auxin flux, the model incorporates a fairly complex feedback mechanism. This is reflected in the nonlinearity of the evolution equations. Numerical solutions to the static version of the model show that it can account for several important features of wood grain, including (1) the apparent "flow" of grain around wounds and knots, (2) the general appearance of grain at branch junctions, and (3) the presence (more accurately, the stability) of circle and X-patterns in whirled grain.

This paper demonstrates that the mechanism of pattern formation in the vascular cambium may be plausibly modeled given our current knowledge of tree biology, but it is only the first step. Values for each of the parameters in the model should be determined empirically. The transverse diffusion constant of auxin in the cambium may be measured using standard radio-label or gas chromatography–mass spectroscopy (GC–MS) techniques (e.g. Uggla, 1998). One likely approach would be to introduce an impediment to the auxin flow and then compare the observed redistribution of auxin to the distribution predicted by computer simulations of the model. The model parameters K and μ will be more difficult to determine, since a direct measurement would ideally require a non-invasive technique for the simultaneous monitoring of auxin concentration and cell orientation in the cambial region. However,

values may be determined indirectly by comparing the measured auxin distribution to recent changes in grain direction as determined by serial sections of the adjacent xylem.

Future refinements to the model may include (1) the effects of mechanical stresses on cambial orientation, (2) the effects of hormones other than auxin, and (3) a more realistic description of the contact-mediated forces between cells.

We are grateful to Michael Bergman, Alan Jones, and James Shinkle for helpful discussions, to James Shinkle for the opportunity to conduct auxin transport experiments at Trinity University, and to Simon's Rock College for the support of this research through the provision of a Faculty Development fund.

REFERENCES

Baier, H. & Bonhoeffer, F. (1992). Axon guidance by gradients of a target-derived component. *Science* **255,** 472–475.

Benedek, G. B. & Villars, F. M. H. (2000). *Physics with Illustrative Examples from Medicine and Biology: Statistical Physics*. New York, NY: AIP Press.

De Gennes, P. G. (1995). *The Physics of Liquid Crystals*. New York, NY: Oxford University Press.

Edelstein-Keshet, L. & Bard Ermentrout, G. (1990). Models for contact-mediated pattern formation: cells that form parallel arrays. *J. Math. Biol*. **29,** 33–58.

Goldsmith, M. H. M. (1977). The polar transport of auxin. *Ann. Rev. Plant Physiol*. **28,** 439–478.

Goldsmith, M. H. M., Goldsmith, T. H. & Martin, M. H. (1981). Mathematical analysis of the chemosmotic polar diffusion of auxin through plant tissues. *Proc. Natl Acad. Sci. U.S.A*. **78,** 976–980.

Green, P. B. (1999). Expression of pattern in plants. *Am. J. Bot*. **86,** 1059–1076.

Harris, J. M. (1969). On the causes of spiral grain in corewood of radiata pine. *N. Z. J. Bot*. **7,** 189–213.

Harris, J. M. (1973). Spiral grain and xylem polarity in radiata pine: microscopy of cambial reorientation. *N. Z. J. For. Sci*. **3,** 363–378.

Harris, J. M. (1981). Spiral grain formation. In: *Xylem Cell Development* (Barnett, J., ed.), pp. 256–274. Kent, U.K.: Castle House Publications.

Harris, J. M. (1989). *Spiral Grain and Wave Phenomena in Wood Formation*. New York, NY: Springer-Verlag.

Hejnowicz, Z. (1973). Morphogenetic waves in cambia of trees. *Plant Sci. Lett*. **1,** 359–366.

Hollis, C. A. & Tepper, H. B. (1971). Auxin transport within intact dormant and active white ash shoots. *Plant Physiol*. **48,** 146–149.

Iqbal, M. (ed.) (1990). *The Vascular Cambium*. New York, NY: John Wiley & Sons.

Jacobs, W. (1952). The role of auxin in differentiation of xylem around a wound. *Am. J. Bot*. **39,** 301–309.

Jacobs, M. & Gilbert, S. F. (1983). Basal localization of the presumptive auxin transport carrier in pea stem cells. *Science* **220,** 1297–1300.

Kirschner, H., Sachs, T. & Fahn, A. (1971). Secondary xylem reorientation as a special case of vascular tissue differentiation. *Israel J. Bot*. **20,** 184–198.

Kramer, E. M. (1999). Observation of topological defects in the xylem of *Populus deltoides* and implications for the vascular cambium. *J. theor. Biol*. **200,** 223–230.

Kramer, E. M. (2001). A mathematical model of auxin-mediated radial growth in trees. *J. theor. Biol*. **208,** 387–397, doi:10.1006/jtbi.2000.2220.

Lachaud, S. & Bonnemain, J. L. (1982). Xylogenese chez les dicotyledones arborescentes. III. Transport de l'auxine et activite cambaile dans les jeunes tiges de Hetre. *Can. J. Bot*. **60,** 869–876.

Lachaud, S. & Bonnemain, J. L. (1984). Seasonal variations in the polar-transport pathways and retention sites of [3H]indole-3-acetic acid in young branches of *Fagus sylvatica* L. *Planta* **161,** 207–215.

Larson, P. R. (1994). *The Vascular Cambium*. New York, NY: Springer-Verlag.

Lev-Yadun, S. & Aloni, R. (1990). Vascular differentiation in branch junctions of trees. *Trees* **4,** 49–54.

Little, C. H. A. (1981). Effect of cambial dormancy state on the transport of [1-^{14}C]indol-3-ylacetic acid in *Abies balsamea* shoots. *Can. J. Bot*. **59,** 342–348.

Little, C. H. A. & Pharis, R. P. (1995). Hormonal control of radial and longitudinal growth in the tree stem. In: *Plant Stems: Physiology and Functional Morphology* (Gartner, B., ed.), pp. 281–319. New York, NY: Academic Press.

Little, C. H. A. & Savidge, R. A. (1987). The role of plant growth regulators in forest tree cambial growth. *Plant Growth Regul*. **6,** 137–169.

Lomax, T. L., Mehlhorn, R. J. & Briggs, W. R. (1985). Active auxin uptake by zucchini membrane vesicles: quantitation using ESR volume and ΔpH determinations. *Proc. Natl Acad. Sci. U.S.A*. **82,** 6541–6545.

Lomax, T. L., Muday, G. K. & Rubery, P. H. (1995). Auxin transport. In: *Plant Hormones: Physiology, Biochemistry, and Molecular Biology* (Davies, P., ed.), pp. 509–530. The Netherlands, Dordrecht: Kluwer Academic Publishers.

Mattheck, C. & Kubler, H. (1995). *Wood: The Internal Optimization of Trees*. New York, NY: Springer-Verlag.

Mitchison, G. J. (1980). The dynamics of auxin transport. *Proc. R. Soc. London, Ser.* B **209,** 489–511.

Mitchison, G. J. (1981). The effect of intracellular geometry on auxin transport II. Geotropism in shoots. *Proc. R. Soc. London Ser.* B **214,** 69–83.

Mogilner, A. & Edelstein-Keshet, L. (1995). Selecting a common direction I. How orientational order can arise from simple contact responses between interacting cells. *J. Math. Biol*. **33,** 619–660.

Mogilner, A. & Edelstein-Keshet, L. (1996). Spatio-angular order in populations of self-aligning objects: formation of oriented patches. *Physica D* **89,** 346–367.

Morgan, F. (1998). *Reimannian Geometry: A Beginners Guide*. Wellesley, MA: A. K. Peters.

Odani, K. (1985). Indole-3-acetic acid transport in pine shoots under the stage of true dormancy. *J. Jpn. For. Soc*. **67,** 332–334.

ONSAGER, L. (1949). The effects of shape on the interaction of colloidal particles. *Ann. N.Y. Acad. Sci*. **51,** 627–659.
PARENT, C. & DEVREOTES, P. (1999). A cells sense of direction. *Science* **284,** 765–770.
PRESS, W., FLANNERY, B., TEUKOLSKY, S. & VETTERLING, W. (1989). *Numerical Recipes*. New York, NY: Cambridge University Press.
RAVEN, J. A. (1975). Transport of indoleacetic acid in plant cells in relation to pH and electrical potential gradients, and its significance for polar IAA transport. *New Phytol*. **74,** 163–172.
ROMBERGER, J. A., HEJNOWICZ, Z. & HILL, J. F. (1993). *Plant Structure: Function and Development*. New York, NY: Springer-Verlag.
RUBERY, P. H. & SHELDRAKE, A. R. (1974). Carrier-mediated auxin transport. *Planta* **118,** 101–121.
SACHS, T. (1969). Polarity and the induction of organized vascular tissues. *Ann. Bot*. **33,** 263–275.
SACHS, T. (1981). The controls of the patterned differentiation of vascular tissues. *Adv. Bot. Res*. **9,** 151–262.
SACHS, T. (1991). *Pattern Formation in Plant Tissues*. New York, NY: Cambridge University Press.
SACHS, T. (2000). Integrating cellular and organismic aspects of vascular differentiation. *Plant Cell Physiol*. **41,** 649–656.
SACHS, T. & COHEN, D. (1982). Circular vessels and the control of vascular differentiation in plants. *Differentiation* **21,** 22–26.
SAVIDGE, R. A. (1996). Xylogenesis, genetic and environmental regulation. *IAWA J*. **17,** 269–310.
SUNDBERG, B. & UGGLA, C. (1998). Origin and dynamics of indoleacetic acid under polar transport in *Pinus sylvestris*. *Phys. Plant*. **104,** 22–29.
SUNDBERG, B., LITTLE, C. H. A., CUI, K. & SANDBERG, G. (1991). Level of endogenous indole-3-acetic acid in the stem of *Pinus sylvestris* in relation to the seasonal variation of cambial activity. *Plant, Cell, Environ*. **14,** 241–246.
UGGLA, C. (1998). Thesis, Swedish University of Agricultural Sciences.
UGGLA, C., MELLEROWICZ, E. & SUNDBERG, B. (1998). Indole-3-acetic acid controls cambial growth in Scots pine by positional signalling. *Plant Physiol*. **117,** 113–121.
VROEGE, G. J. & LEKKERKERKER, H. (1992). Phase transitions in lyotropic colloidal and polymer liquid crystals. *Rep. Prog. Phys*. **55,** 1241–1309.
WILSON, B. F., WODZICKI, T. J. & ZAHNER, R. (1966). Differentiation of cambial derivatives: proposed terminology. *For. Sci*. **12,** 438–440.
ZAGORSKA-MAREK, B. & LITTLE, C. H. A. (1986). Control of fusiform initial orientation in the vascular cambium of *Abies balsamea* stems by indole-3-ylacetic acid. *Can. J. Bot*. **64,** 1120–1128.
ZAJACZKOWSKI, S., HEJNOWICZ, Z. & ROMBERGER, J. (1984). Auxin waves and plant morphogenesis. In: *Encyclopedia of Plant Physiology New Series,* (Scott, T., ed.), Vol. 10 pp. 244–262. New York, NY: Springer-Verlag.
ZAMSKI, E. & WAREING, P. F. (1974). Vertical and radial movement of auxin in young sycamore plants. *New Phytol*. **73,** 61–69.

Appendix A

Derivation of eqn (1)

In this appendix, we follow the approach of Mitchison (1980), and adopt his notation. Consider a homogeneous file of meristem cells aligned end to end. The flux of auxin through the file is denoted by ϕ. Mitchison assumes that (1) auxin is free to diffuse through the interiors of cells, and (2) the flux of auxin between adjacent cells satisfies the form

$$\phi = pa_1 + q(a_1 - a_2), \qquad \text{(A.1)}$$

where a_1 and a_2 are the concentrations of auxin on either side of the interface between cells, and p and q are constants. [The interface of Mitchison includes the cell wall and cell membranes. Goldsmith *et al.* (1981) includes the tonoplast as well].

We assume the fractional change in flux between adjacent cells is much less than 1. The specific condition is $(\mathrm{d}\phi/\mathrm{d}x)(L/\phi) \ll 1$, where L is the length of one cell. Figure A1 shows four adjacent cells in the file. The flux of auxin through the cytoplasm is $\phi = -D(\mathrm{d}a/\mathrm{d}x)$ where D is the diffusion constant. Since the flux is approximately constant across neighboring cells, the concentration a is a linear function of position within each cell and

$$\phi = const. = -D\frac{a_1 - a_0}{L} = -D\frac{a_3 - a_2}{L}. \qquad \text{(A.2)}$$

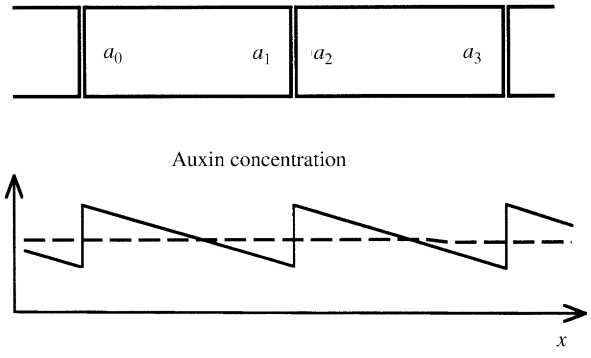

FIG. A1. Top: Sketch of four meristem cells, as described in the text. Labeled auxin concentrations, a_j, are those immediately adjacent to the interfaces. Bottom: Sketch of the intracellular auxin concentration as a function of position (——), and the smoothed auxin concentration (- - - - -). Direction of active transport is to the right.

Also, the mean concentration of auxin in each cell is just the average of the endpoint values,

$$\bar{a}_L = (a_0 + a_1)/2 \quad \text{and} \quad \bar{a}_R = (a_2 + a_3)/2, \quad \text{(A.3)}$$

where the subscripts L and R denote the left and right cells shown in the figure. Combining eqns (A.1)–(A.3), we can rewrite the flux in terms of the means

$$\phi = -D_{eff}\,\frac{\bar{a}_R - \bar{a}_L}{L} + v\,\frac{\bar{a}_R + \bar{a}_L}{2}, \quad \text{(A.4)}$$

where

$$D_{eff} = \frac{L(p/2 + q)}{1 + (L/D)(p/2 + q)}$$
$$v = \frac{p}{1 + (L/D)(p/2 + q)}. \quad \text{(A.5)}$$

The first term on the right-hand side of eqn (A.4) looks like Fick's law, with an effective diffusion constant D_{eff}. The second term looks like a transport velocity v times the mean auxin concentration. Our expression for the transport velocity, eqn (A.5), is identical to that found by Mitchison (1980) using a more rigorous approach.

Equation (A.4) is the discrete form of the flux equation that combines active transport with diffusion (Benedek & Villars, 2000). The continuous version is our eqn (1). The inclusion of additional cellular compartments and membranes (as in Goldsmith *et al.*, 1981) will complicate the calculation of D_{eff} and v, but eqn (1) is unchanged.

Appendix B

Computer Simulation Techniques

Our simulations used a Forward Time, Centered Space (FTSC) algorithm as described in Chap. 17 of Press *et al.* (1989). The fields $m(x, y)$ and $\phi(x, y)$ were discretized on a square lattice with spacing $\Delta x \leqslant 0.2$ mm. To find the static solution, we evolved the *time-dependent* equations, (5), (6), and (9), until the fields stopped changing significantly. The initial condition was typically a uniform distribution for ϕ and m, plus a small amount of randomness. This technique converged to a static solution after 4000–8000 iterations (a few minutes on a Macintosh G3).